water

MDPI

Article

On the Use of Weather Generators for the Estimation of Low-Frequency Floods under a Changing Climate

Carles Beneyto, José Ángel Aranda * and Félix Francés

Research Institute of Water and Environmental Engineering (IIAMA), Universitat Politècnica de València, Camino de Vera s/n, E-46022 Valencia, Spain; carbeib@upv.edu.es (C.B.); ffrances@upv.es (F.F.)
* Correspondence: jaranda@upv.es; Tel.: +34-963-877-000 (ext. 76152)

Abstract: The present work presents a methodology based on the use of stochastic weather generators (WGs) for the estimation of high-return-period floods under climate change scenarios. Applying the proposed methodology in a case study, Rambla de la Viuda (Spain), satisfactory results were obtained through the regionalization of the bias-corrected EUROCORDEX climate projections and the integration of this information into the parameterization of the WG. The generated synthetic data series fed a fully distributed hydrological model to obtain the future flood quantiles. The results obtained show a clear increase in the precipitation extreme quantiles for the two analyzed projections. Although slightly reducing the annual amount of precipitation, variations between 4.3% for a return period of 5 years in the mid-term projection and 19.7% for a return period of 100 years in the long-term projection have been observed. In terms of temperatures, the results point to clear increases in the maximum and minimum temperatures for both projections (up to 3.6 °C), these increases being greater for the long-term projection, where the heat waves intensify significantly in both magnitude and frequency. Finally, although rivers may present, in general, with lower flows during the year, flood quantiles experience an increase of 53–58% for high return periods, which reach values of up to 145% when we move to smaller catchments. All this combined translates into substantial shifts in the river flow regimes, increasing the frequency and magnitude of extreme flood events.

Keywords: weather generator; climate change; quantile; regional extreme precipitation study

Citation: Beneyto, C.; Aranda, J.Á.; Francés, F. On the Use of Weather Generators for the Estimation of Low-Frequency Floods under a Changing Climate. *Water* **2024**, *16*, 1059. https://doi.org/10.3390/w16071059

Academic Editor: Pavel Groisman

Received: 14 March 2024
Revised: 29 March 2024
Accepted: 4 April 2024
Published: 6 April 2024

1. Introduction

Ensuring the accurate estimation of high-return-period flood quantiles is paramount for appropriately dimensioning infrastructure and establishing effective flood warning systems [1,2]. Despite the emergence of novel methodologies for estimating these quantiles in recent years, the prevailing estimates still harbor substantial uncertainties. The limited temporal length of available time series data and the sparse deployment of rain gauges and monitoring stations stand out as primary sources of uncertainty, presenting formidable challenges within Flood Frequency Analysis (FFA). This challenge is particularly accentuated in arid and semi-arid regions [3], which are often poorly monitored.

Rapid advancements in computing capabilities have paved the way for the widespread adoption of Synthetic Continuous Simulation (SCS) within the scientific community: a hybrid methodology blending statistical and deterministic techniques for FFA studies. Leveraging a stochastic weather generator (WG) in tandem with a hydrological model (HM), SCS facilitates the generation of synthetic data series spanning a wide range of hydrometeorological variables. However, to ensure the robust performance of WGs, it is necessary to feed them with adequate input information, particularly when modeling extreme events [4]. Nevertheless, the duration of current observational records, typically limited to around 100 years at most, proves insufficient for optimal WG performance. Consequently, addressing this data deficiency necessitates the incorporation of additional flood information [5,6]. This may encompass non-systematic data sources, including

historical and palaeoflood records, as demonstrated by Benito et al. [7], regional maximum precipitation studies, as exemplified by Evin et al. [8], or a blend of both approaches, as showcased by Beneyto et al. [9].

Furthermore, climate studies predict an increase in the frequency and magnitude of extreme events (e.g., [10,11]), which, combined with the global socioeconomic development, will lead to an increase in flood losses resulting from extreme precipitation events in the near future [12]. All this further highlights the need to develop methodologies that reduce the uncertainty in the flood estimates, especially those associated with a low probability of occurrence. Generally, most of the studies currently carried out to estimate future flood quantiles are broadly based on the use of the available products from Global Circulation Models (GCMs), downscaling the outputs of these to finer scales and obtaining the flow series through an HM (e.g., [13–15]). Downscaling methods to obtain observed small-scale variables and those from GCMs can be based on the use of either RCMs, analog methods (circulation typing), regression analysis, or neural network methods [16]. However, downscaled data present large biases that need to be corrected. Over the past decades, various bias correction methods have been proposed. Main examples include delta change [17,18], direct statistical downscaling [19,20], quantile mapping (QM) [21], Nested Bias Correction or its multivariate counterpart Multivariate Bias Correction [22]. A more extensive review of bias correction methods can be found in Themeßl et al. [23] and Maraun [24].

Although it is true that to properly capture extreme convective precipitation episodes a sub-daily modeling time step is required for most applications [25], and that climate model outputs are now increasingly available at sub-daily time steps, a very limited number of studies have looked at the bias correction of sub-daily climate model outputs [26] and the focus has been on correcting sub-daily annual maximum values (e.g., [27]). Instead, daily climate projections of 30 years in length are usually used in climate change studies that, although according to the "World Meteorological Organization", are of sufficient length to smooth out the variations from one year to the next [28], in the opinion of the authors of this work, they are insufficient for the adequate estimation of extreme flood quantiles. In fact, in the analysis conducted by Beneyto et al. [29], in which different sample data lengths (i.e., 60, 90, and 120 years) were analyzed, it was concluded that no significant reduction in the uncertainty of the estimations was found compared to the reduction obtained when incorporating additional information. Although a 30-year data series could be enough for specific studies and some meteorological variables, flood quantile estimation requires longer datasets, especially if we are focused on adequately modeling extreme events, which could be achieved with an effectively parametrized WG.

In this context and following the steps of the previous works of Beneyto et al. [9,29,30], this study presents a new methodology that integrates different sources of information generated from hydrometeorological models fed with the amount of information necessary to achieve an adequate characterization of the main variables that must be considered in the FFA under climate change scenarios of only 30 years in length. This methodology has been applied in a case study: Rambla de la Viuda (Spain) (Figures 1 and 2).

Building upon previous research, this study addresses the critical gap in flood estimation methodologies by proposing an innovative approach that integrates diverse sources of hydrometeorological information. By leveraging this approach, which focuses on accurately characterizing key variables within the FFA under climate change scenarios, this study contributes significantly to enhancing the precision and reliability of flood quantile estimations. Unlike previous studies limited by short observational records and methodological constraints, this research provides a novel framework capable of effectively utilizing climate data spanning just 30 years, thereby offering a practical solution to the pressing need for improved flood risk assessment in the face of evolving climatic conditions.

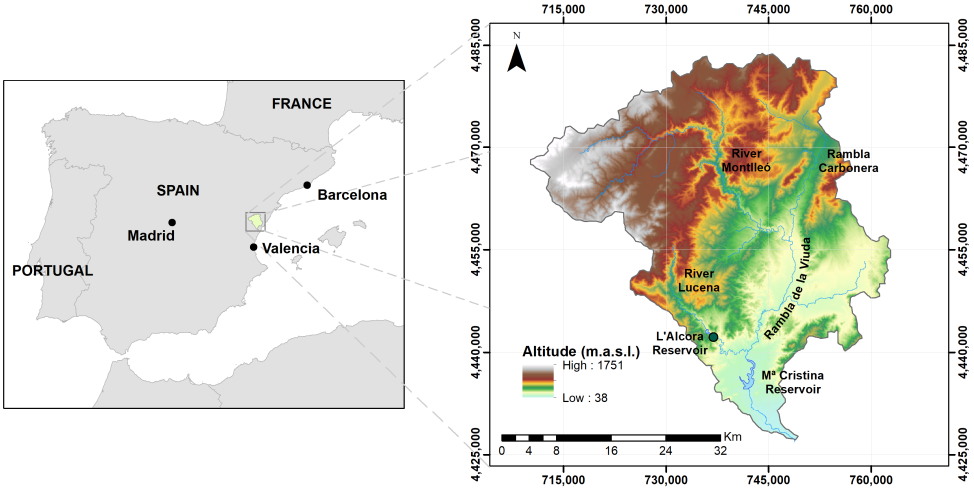

Figure 1. Study area.

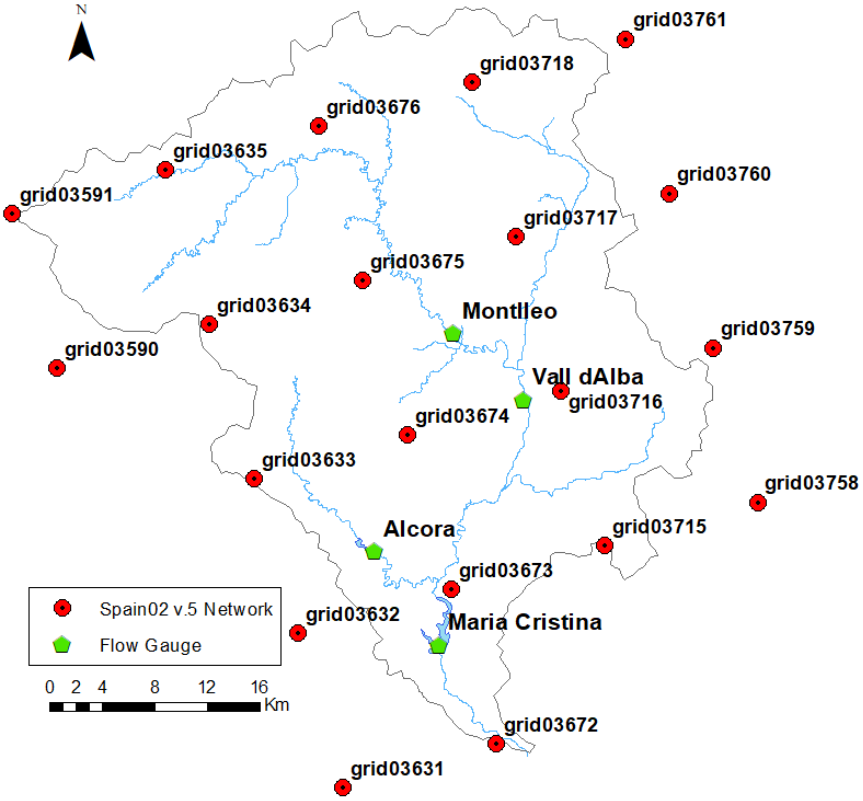

Figure 2. Hydrometeorological information.

2. Case Study

2.1. Study Area

The methodology outlined in this study was implemented and evaluated in the setting of the Rambla de la Viuda (Castellón), a typical Mediterranean ephemeral river located in eastern Spain (Figure 1). Stretching over a distance of 36 km and covering a drainage area of 1513 square kilometers, this river originates from the junction of the Montlleó River and the Rambla Carbonera, eventually joining the Millars River near its endpoint at the Mediterranean Sea.

Annual precipitation averages approximately 550 mm, although the majority of this rainfall is concentrated in isolated episodes, especially during the autumn months, associated with mesoscale convective systems. Consequently, the river sustains flow for an

average of 31 days annually, often persisting for as briefly as 2 or 3 days, and is correlated with cumulative rainfall surpassing 70 mm [31].

2.2. Hydrometeorological Information

Meteorological data were obtained from different sources. Observed daily precipitation and maximum and minimum temperatures were obtained from the Spain02-v5 dataset [32,33]. A total of 20 pluviometers and thermometers covering the basin with daily records from 1951 to 2015 (66 years) were selected (Figure 2).

Climate projections were obtained from the "Coordinated Regional Downscaling Experiment for Europe" experiment (EURO-CORDEX) (https://www.euro-cordex.net/ (accessed on 15 February 2024)). A total of 12 different combinations of Global Circulation Models (GCMs) and Regional Circulation Models (RCMs) were used in this study (Table 1), including daily precipitation and minimum and maximum temperature with a spatial resolution of 0.11°. These data included a control period (1971–2000), a medium-term projection (2035–2064), and a long-term projection (2065–2094). The projections used in this study correspond to the Radioactive Concentration Pathway (RCP) 8.5, which represents a scenario with continuous emissions of CO_2 throughout the 21st century [34]. Additionally, temperature data (bias-corrected) were used to create time series of Potential Evapotranspiration (ET0), which were estimated with the Hargreaves–Samani equation [35].

Table 1. EUROCORDEX models.

Model	GCM	RCM	Institute
1	MPI-M-MPI-ESM-LR	COSMO-crCLIM-v1-1	CLMcom-ETH
2	CNRM-CERFACS-CNRM-CM5	CCLM4-8-17	CLMcom
3	CNRM-CERFACS-CNRM-CM5	RACMO22E	KNMI
4	ICHEC-EC-EARTH	COSMO-crCLIM-v1-1	CLMcom-ETH
5	ICHEC-EC-EARTH	RACMO22E	KNMI
6	IPSL-IPSL-CM5A-MR	RACMO22E	KNMI
7	MOHC-HadGEM2-ES	CCLM4-8-17	CLMcom
8	MOHC-HadGEM2-ES	RACMO22E	KNMI
9	MPI-M-MPI-ESM-LR	CCLM4-8-17	CLMcom
10	MPI-M-MPI-ESM-LR	KNMI-RACMO22E	KNMI
11	MPI-M-MPI-ESM-LR	REMO2009	MPI-CSC
12	NCC-NorESM1-M	COSMO-crCLIM-v1-1	CLMcom-ETH

Lastly, discharge data for the HM implementation were obtained from the Júcar River Basin Water Authority (CHJ) through its Automatic System of Hydrological Information (SAIH): two gauges located at Vall d'Alba and Montlleó Rivers; and two stations located in Alcora and Maria Cristina reservoirs, where the flows were estimated from the balance between the reservoir levels and their releases.

3. Methodology

Following in the footsteps of a previous work by Beneyto et al. [9], the proposed methodology encompasses undertaking the following procedures: (1) correct the bias of climate models; (2) perform (if not available) a regional study of maximum daily precipitation of the bias-corrected climate models (both for control period and for the projections); (3) implement a stochastic multi-site WG incorporating the information from the ad hoc regional studies and generate very long series (i.e., 5000 years) of precipitation and temperatures; and (4) implement a fully distributed HM and feed it with the outputs from the WG to generate series of synthetic discharges. Figure 3 shows an outline of the proposed methodology, the steps of which are developed in the following sections.

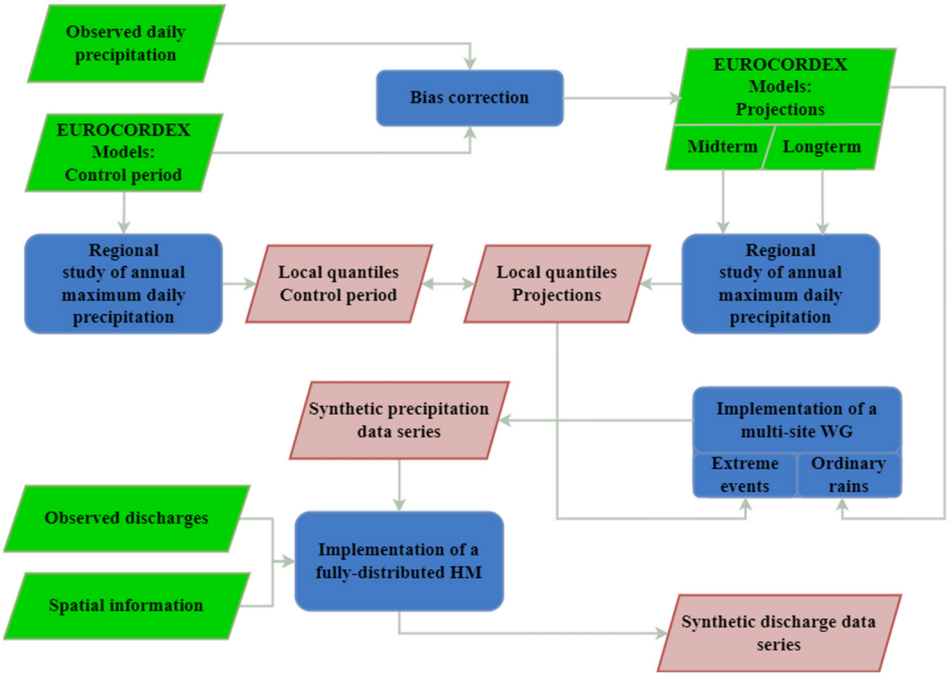

Figure 3. Workflow chart of the proposed methodology.

3.1. Bias Correction of Climate Series

The temperature and precipitation time series of the 12 climate models were bias-corrected relative to the observed climate data (Spain02 dataset). The bias correction was based on the non-parametric statistical transformation of empirical quantiles or "quantile mapping" [36] and was implemented for each season of the year separately (December–February, March–May, June–August, and September–November). The bias correction procedure applied in this study also considered the adaptation of the frequency of wet/dry days proposed by Themeßl et al. [23]. Bias correction functions established in the control period were applied to future climate projections assuming stationary biases.

3.2. Regional Study of Maximum Daily Precipitation

The second phase of the methodology, if not available, entails conducting a comprehensive regional study of maximum daily precipitation, encompassing both historical control period data and projections previously bias-corrected. This in-depth analysis aims to expand the available information and capture a holistic understanding of precipitation patterns across the region. The insights gleaned from this study serve as crucial inputs for the effective implementation of the WG, which is explained in the following subsection. A comparison of regionalization methods to improve in situ estimates of daily precipitation can be found in Haruna et al. [37].

In our study, the regional analysis followed the methodology developed by Hosking and Wallis [38,39], employing the Index Variable method [40] alongside linear moments. As recommended by the authors, a Discordance and Homogeneity test based on L-moments was conducted to identify homogeneous regions, resulting in the identification of a single homogeneous region.

Finally, once the homogeneous regions were identified and following the premise of the Index Variable, the probability function that best fit (i.e., Generalized Pareto Distribution) was selected according to the criterion developed by Akaike [41] and the local quantiles were deregionalized for each of the models and grids of the basin.

3.3. Weather Generator: GWEX

The WG employed in this study was GWEX [8], a multi-site stochastic model designed specifically to accurately model extreme events. Noteworthy among its many features is

the incorporation of the Extended Generalized Pareto Distribution (E-GPD) function, as described by Papastathopoulos and Tawn [42]. This distribution is essentially derived by raising the Generalized Pareto Distribution to a power $k > 0$. This unique characteristic enhances the WG's capability to effectively simulate extreme weather phenomena, which is particularly relevant for the objectives outlined in this study.

$$F(x;\lambda) = \left[1 - \left(1 + \frac{\xi x}{\sigma}\right)_{+}^{-1/\xi}\right]^{\kappa}, \quad x > 0 \tag{1}$$

The parameter vector $\lambda = (k, \sigma, \xi)$ comprises the parameters controlling various aspects of the distribution. Specifically, k, governs the shape of the lower tail, σ represents the scale parameter, and ξ regulates the decay rate of the upper tail, as described by Naveau [43]. In a similar way to the proposed methodology in Beneyto et al. [9], the value of this latter parameter was adjusted for each model with the regional X_{100}, thus reducing the uncertainty in the estimates as demonstrated in Beneyto et al. [29,30].

3.4. Ecohydrological Model: TETIS

The fully distributed ecohydrological model TETIS was used [44,45]. This model had already been implemented in a previous work by Beneyto et al. [9]. In this study, slight modifications to the correction factors were made, which improved the results in terms of the Nash–Sutcliffe efficiency [46] both in calibration and in temporal, spatial, and spatio-temporal validation. For more information regarding the model's implementation, refer to Beneyto et al. [9].

4. Results

4.1. Temperatures

Although the analysis of the temperatures is not within the main objectives of the present study, it is evident that the potential change in the temperature trends resulting from the effects of climate change will lead to alterations to the discharge regimes. That is, temperature has a clear impact on the initial conditions of the basin: apart from higher evapotranspiration, higher temperatures would potentially increase the soil aridity, resulting in higher volumes of infiltration at the initial moments of the storm, thus, supposedly resulting in lower initial flows.

Figure 4 below shows the comparison of the mean daily maximum and minimum temperatures of the observations and the 12 GCM–RCM combinations for both the mid-term and the long-term projection. It is worth mentioning that, in the case of the temperatures, the analysis has been carried out comparing the data purely from the observations and from the climate projections (bias-corrected). That is, the use of a WG was considered not necessary for this analysis given that the length of the data series was enough to capture the trend and the potential variations.

From this figure, it can be appreciated that there is a clear increasing trend for both the maximum and minimum temperatures for all the projections. This increase ranges from 1.9 °C for the mid-term projection to 3.4 °C for the long-term projection in the case of the minimum temperature and from 2.0 °C to 3.6 °C, respectively, in the case of the maximum temperature. If we look at the monthly variations (Table 2), it can be observed that, for both variables, the greater increases occur over the summer months, whereas the lower increases take place during the winter months.

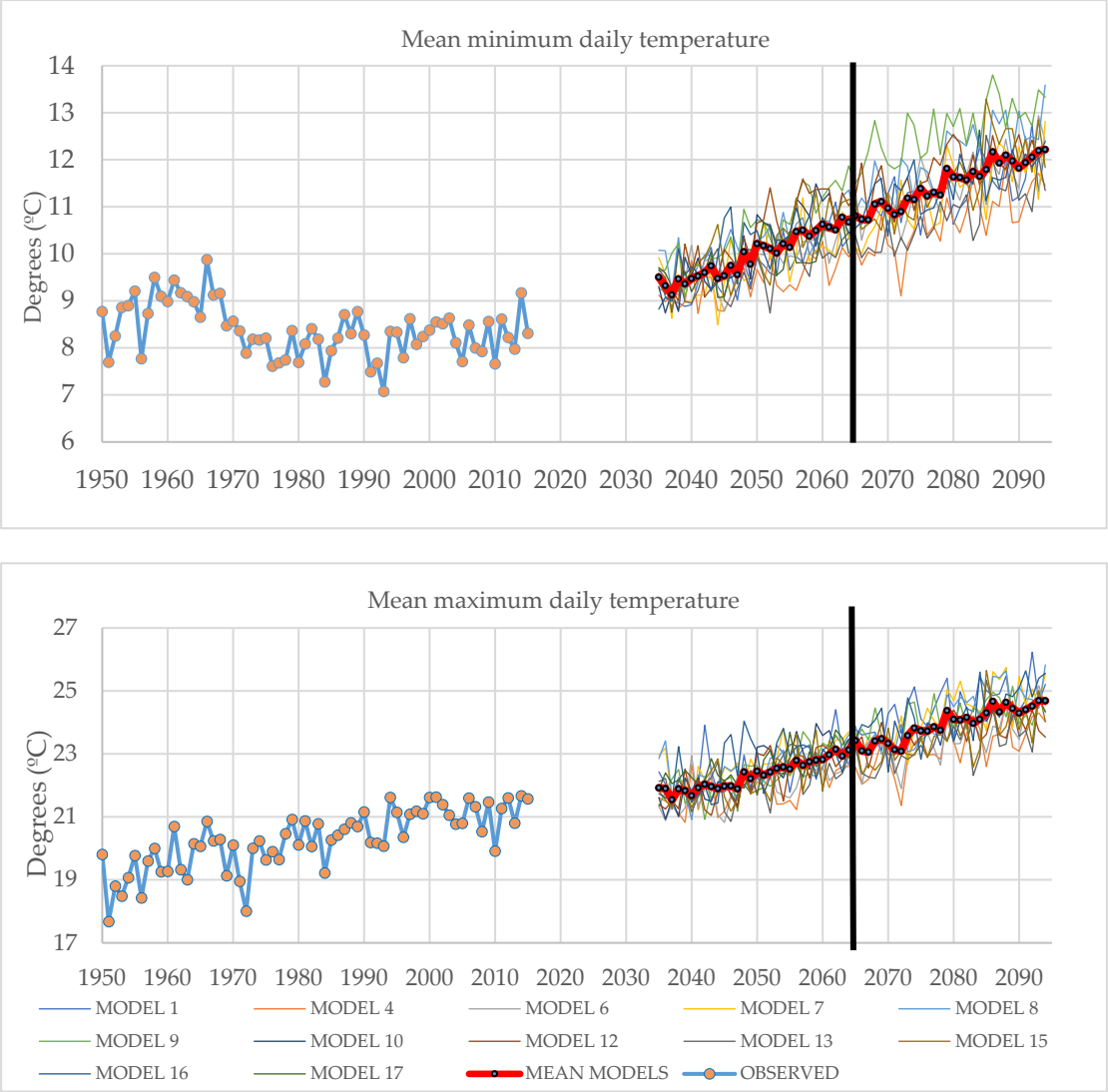

Figure 4. Mean minimum (**top**) and maximum (**bottom**) daily temperature of the observations and the 12 climate projections (black line denotes the separation between mid-term and long-term projections).

Table 2. Average monthly increase in maximum and minimum temperatures for mid-term and long-term projections.

ΔT (°C)	Minimum Temperature		Maximum Temperature	
	Mid-TERM	Long-Term	Mid-Term	Long-Term
January	2.43	2.55	2.25	2.25
February	1.90	1.93	2.17	1.98
March	2.41	2.61	2.27	2.56
April	2.39	2.98	2.76	3.55
May	1.34	2.61	1.51	3.08
June	3.02	5.32	3.34	6.04
July	2.04	5.04	1.80	5.11
August	1.06	4.26	1.35	4.73
September	0.41	3.19	0.34	3.18
October	1.47	3.68	1.43	3.67
November	2.71	4.28	2.73	4.18
December	1.67	2.59	1.56	2.40

Finally, an analysis of the percentage of the days with temperatures under or over certain thresholds was conducted. The results of this analysis are shown in Figure 5 below.

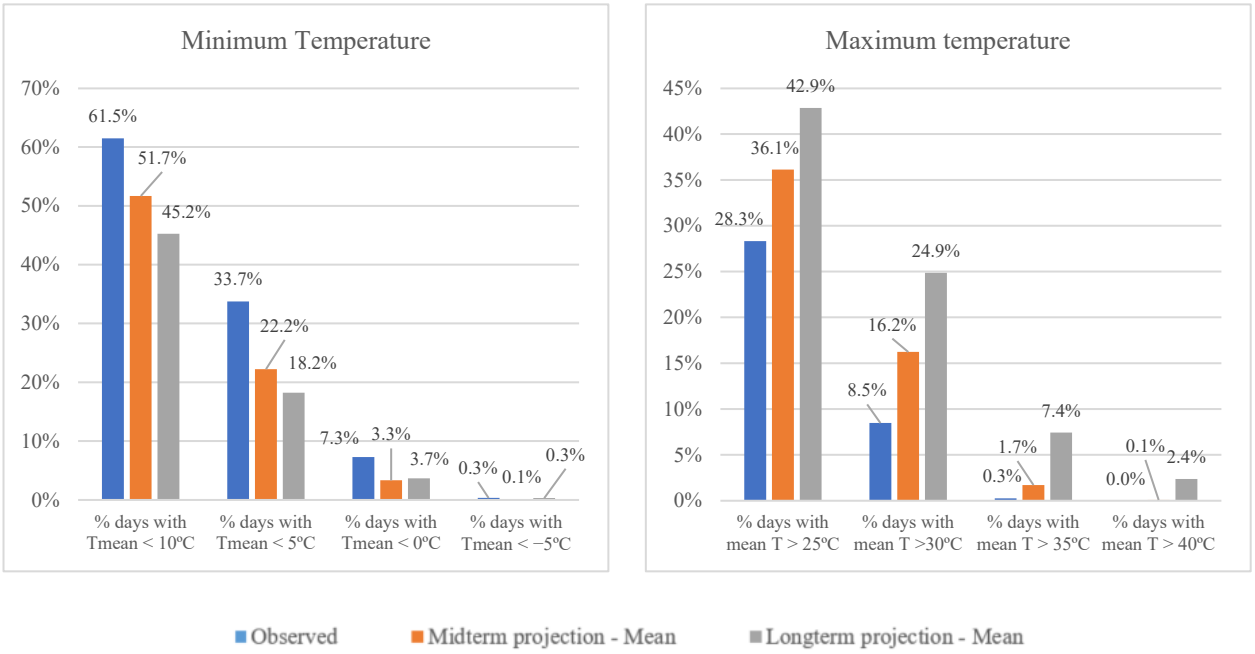

Figure 5. Variation in the number of days with extreme mean daily temperatures.

In the case of the minimum temperature, the percentage of days with a mean minimum temperature lower than 10 °C, 5 °C, 0 °C, and −5 °C was analyzed, observing a clear decrease in the number of cold days compared to the observations and which was more pronounced in the case of the long-term projection. Similarly, in the case of the maximum temperature, the percentage of days with a mean maximum temperature higher than 25 °C, 30 °C, 35 °C, and 40 °C was examined, suggesting a significant increase in the number of warm days and, again, this increase being more marked in the case of the long-term projection.

4.2. Precipitation

The results in terms of the precipitation are shown in Figure 6, where the boxplots of the estimated precipitation quantiles (standardized with the homologous quantiles in the control period) from the 5000 years generated for both the mid-term projection and the long-term projection are represented for one of the grids of the basin (i.e., grid 03759). Similarly to what occurs with the rest of the grids, the low-return-period quantiles experience small differences with their corresponding quantiles in the control period. The future quantiles tend to increase systematically with the return period, this increase being more evident in the case of the long-term projection. Additionally, the uncertainty of these estimations broadens with the quantile (wider boxplots).

Considering the mean quantile of all the grids and all the models (in the control period, mid-term projection, and long-term projection), we could obtain the expected differences in the future quantiles (Δ%), which applies to the observed quantile results in the estimated future precipitation quantiles (Table 3).

These increases in the precipitation quantiles range between 4.3% for a return period of 5 years in the mid-term projection and 19.7% for a return period of 100 years in the long-term projection. While it is clear that the increase is proportional to the return period in the case of the mid-term projection, for the long-term projection, this increase seems to be quite stable for all return periods except for a return period of 5 years.

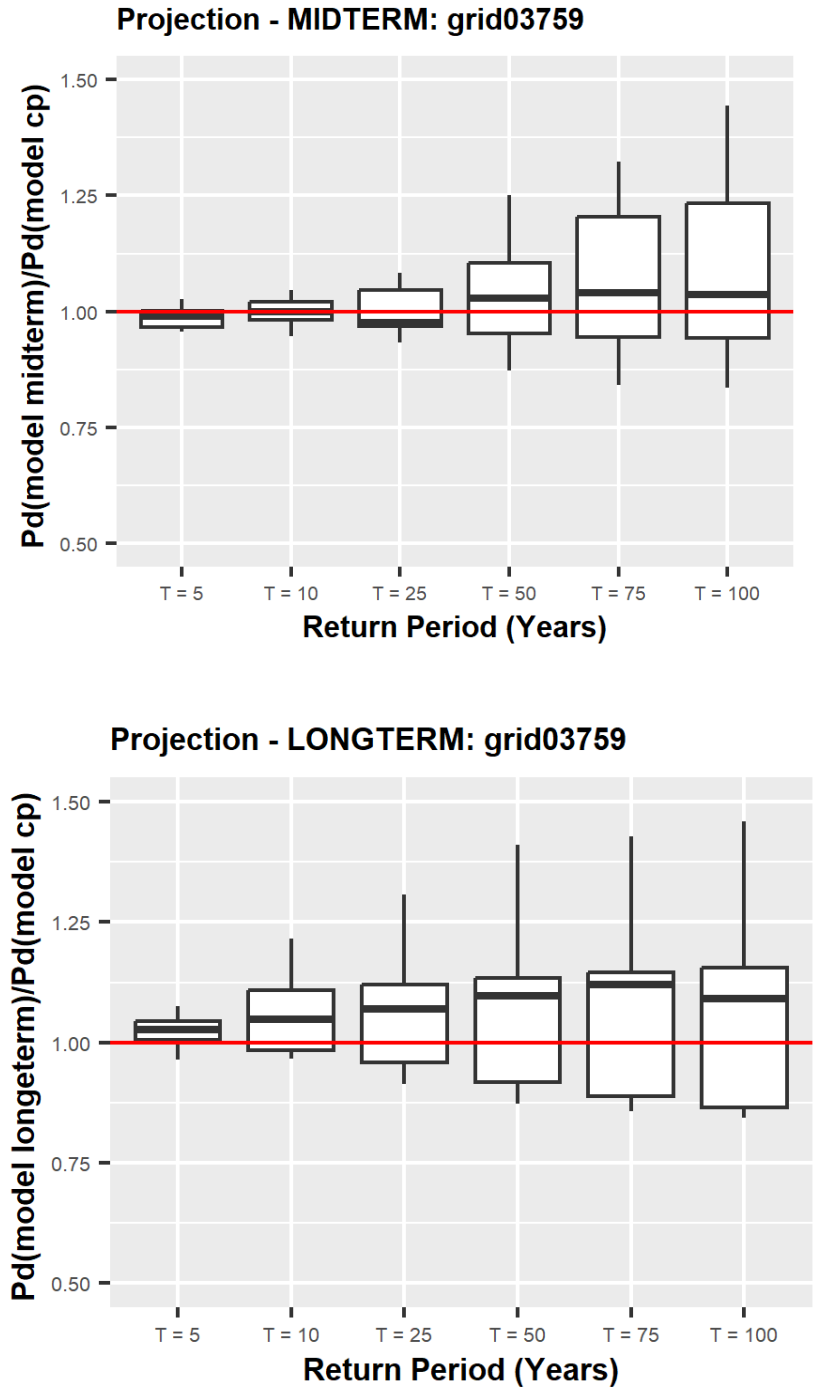

Figure 6. Boxplots of the standardized precipitation quantiles (with the model quantile in control period) in grid03759 for both mid-term projection (**up**) and long-term projection (**down**).

Table 3. Estimated future precipitation quantiles (mean of all models and all grids).

T (Years)	Observations	Mid-Term Projection		Long-Term Projection	
	X_T	Δ%	X_T	Δ%	X_T
5	80	4.3%	83	12.8%	90
10	99	6.0%	105	16.7%	116
25	125	8.4%	136	18.6%	148
50	145	11.5%	162	19.3%	173
75	158	13.5%	179	19.7%	189
100	167	14.4%	191	19.4%	199

4.3. Discharges

The 25 WG implementations (i.e., observations, 12 mid-term projections, and 12 long-term projections) fed the fully distributed HM TETIS, obtaining the discharges shown in Figure 7, represented by their plotting positions obtained with the Cunnane formulation [47].

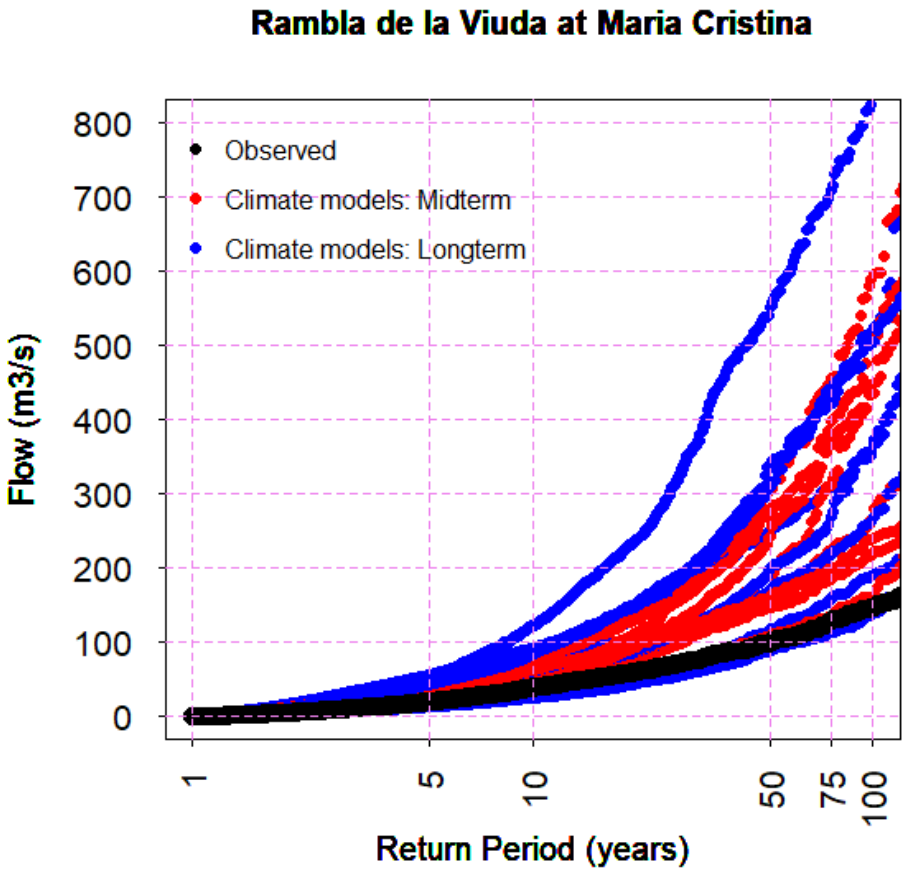

Figure 7. Plotting positions of the observed daily discharges and the simulated discharges from the climate models (both for the mid-term and for the long-term projection) at Maria Cristina reservoir.

As expected with the results obtained for the precipitation, the plotting positions of the generated discharges are clearly higher than those observed for both the mid-term and the long-term projection. Notwithstanding, it is also clear the uncertainty surrounding these estimates depending on the model, presenting flood quantiles that range from 180 m^3/s to 810 m^3/s for a return period of 100 years, for example. Despite variations across scenarios, an increase is evident in all cases; Table 4 presents the estimated percentage increase in the flood quantiles at the Maria Cristina reservoir, calculated as the difference between those obtained during the control period and those projected by each model. Additionally, the table includes the anticipated future flood quantile, derived by applying this percentage increase to the observed quantiles.

The increase is systematic for all the quantiles and for both projections, ranging from 8 to 12% for the low return periods to 53 to 58% for the high return periods, where increases in the flood quantiles are more pronounced. Finally, and exploiting the benefits of using a fully distributed HM, the same analysis was conducted for an additional two flow gauges located at Vall d'Alba (906 km^2) and Montlleó (501 km^2) (Table 5). The results in both flow gauges presented increases for all the flood quantiles; however, it can be observed that, compared to Maria Cristina, these increases are higher in Vall d'Alba (ranging from 10% to 80%) and especially in Montlleó (ranging from 5% to 145%). That is, future flood quantiles appear to exhibit higher increases as the catchment becomes smaller.

Table 4. Estimated future flood quantiles at Maria Cristina (catchment area: 1447 m^2).

T (Years)	Observed (m^3/s)	Δ%	Climate Projections (m^3/s) Mid-Term	Δ%	Long-Term
5	20	12%	22	8%	21
10	38	12%	43	16%	44
25	68	22%	83	33%	91
50	101	38%	140	54%	155
75	130	48%	192	56%	202
100	147	53%	225	58%	232

Table 5. Estimated future flood quantiles at Vall d'Alba and Montlleó (catchment areas: 906 km^2 and 501 km^2, respectively).

Vall d'Alba

T (Years)	Observed (m^3/s)	Δ%	Climate Projections (m^3/s) Mid-Term	Δ%	Long-Term
5	12	11%	14	10%	13
10	22	13%	24	33%	29
25	39	21%	47	64%	64
50	56	41%	79	88%	105
75	69	49%	103	86%	130
100	80	50%	121	80%	145

Montlleó

T (Years)	Observed (m^3/s)	Δ%	Climate Projections (m^3/s) Mid-Term	Δ%	Long-Term
5	4	3%	4	5%	4
10	6	7%	6	42%	8
25	11	27%	14	111%	23
50	17	57%	27	137%	40
75	21	73%	37	145%	52
100	28	77%	49	130%	64

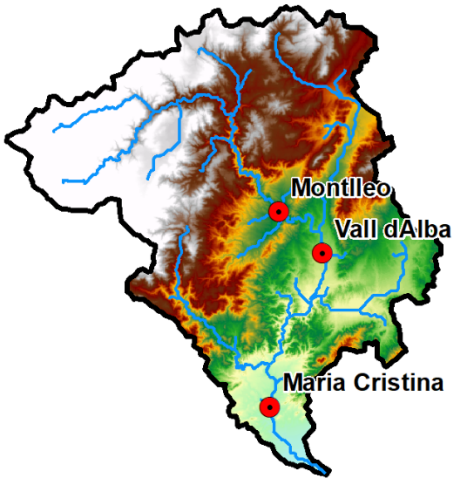

5. Discussion

SCS, a widely embraced hybrid methodology for flood quantile estimations, addresses the limitations of purely statistical or deterministic approaches in estimating flood quantiles. By effectively characterizing the initial conditions of a basin and adequately representing the spatio-temporal distribution of precipitation, SCS offers significant advantages in flood estimation [48]. Despite these advancements, uncertainty persists in estimating low-frequency flood quantiles.

The primary source of this uncertainty stems from the length of existing hydrometeorological series and the sparse distribution of monitoring stations [49], particularly pronounced in arid and semi-arid regions. The scarcity of data poses a formidable challenge in accurately estimating flood quantiles. While longer input data sets could potentially mitigate uncertainty, this remedy relies solely on the passage of time for data accumulation.

Addressing the challenges of uncertainty in flood quantile estimation requires concerted efforts in data collection and analysis [50]. Strategies to enhance monitoring networks and extend data collection periods can contribute to reducing uncertainty [51]. Additionally, advancements in modeling techniques and the integration of remote sensing data can provide valuable insights into hydrological processes [52], aiding in more accurate flood quantile estimation. Despite the inherent challenges, ongoing research and technological innovations hold promise for improving the reliability of flood quantile estimates and enhancing our ability to manage flood risks effectively. Additionally, climate patterns are no longer as we used to know them; they are rapidly changing as a consequence of the effects of climate change. Practically all the available research points to alterations in

river flow regimes resulting from the changes in temperature and precipitation patterns (e.g., [53–55]). This adds even more uncertainty to the estimation of future flood quantiles, and is certainly a challenge to be faced for the correct sizing of infrastructures and for protecting those areas now vulnerable to being affected by floods.

Numerous studies can be found in the literature assessing the impacts of climate change on hydrology and water resources in many regions (e.g., [56–58]). They all start from the same source of information: GCMs. These are the most advanced tools currently available for simulating the response of the global climate system to increasing greenhouse gas concentrations [59]. Notwithstanding, these models inevitably simulate large biases in temperature, precipitation, and humidity at regional scales and at individual grid points [60,61] and their resolution is too coarse for undertaking reliable flood studies at a local scale. Downscaling methods to obtain observed small-scale variables and from GCMs can be based on the use of either RCMs, analogue methods (circulation typing), regression analysis, or neural network methods [16].

Many projects are now under way, offering a wide range of climatic data, mostly based on combinations of GCMs and RCMs, such as the EUROCORDEX project, the data of which have been used in the present study. These climate projections include a 66-year control period for correcting the potential biases and 95 years of future projections. Although 95 years could be a reasonable data length for certain studies employing specific climatic variables, in the opinion of these authors, it is not enough in the case of precipitation, specifically if we are focusing on estimating extreme events. WGs, however, fed by these climate projections, can generate long data series in multiple realizations, reducing the uncertainty of future quantile estimations. Nevertheless, it has been demonstrated that WGs need robust information to perform adequately [9,29,30]. Incorporating additional sources of information or improving model implementation can lead to considerable improvements in the reliability of flood quantile estimates.

The present work tries to contribute in this sense, establishing a new methodology for the estimation of extreme floods in climate change scenarios through the use of WGs. Similarly as in Beneyto et al. [9,29,30], we perform an ad hoc regional study of the annual maximum daily precipitation, the results of which are incorporated in the WG parametrization for better reproduction of the precipitation quantiles in both the present and the future climate.

The results obtained applying this methodology in terms of temperatures show a substantial increase in relation to current observations for both the medium-term projection (35–64) and the long-term projection (65–94), with the increase being considerably greater for the long-term projection, with mean maximum temperature values of up to 6 °C higher for the month of June. These results follow the same trend as the results obtained by other authors such as Wuebblles et al. [62] or Zubaidi et al. [63], predicting warmer summers and milder winters. Furthermore, as can be seen in Figure 5, the number of days with a mean maximum temperature above 35 °C and 40 °C increases considerably, which means that the number of heat waves will intensify in the future, as other studies have already highlighted (e.g., [64,65]). Similarly, the mean minimum temperature also increases in both projections, although this is slightly less pronounced than in the case of the maximum temperature. Furthermore, the percentage of intense cold days reduces systematically for all the analyzed temperatures in the case of the medium-term projection, although it increases again for the long-term projection when looking at a mean temperature below 0 °C and −5 °C, which means that cold waves could intensify in the future, even though this increase could also be caused by the models' variability.

When we look at the precipitation, the results obtained show a substantial increase for all quantiles, both in the medium-term projection (35–64) and in the long-term projection (65–94) with respect to the control period regional quantiles. Despite the higher variability between the models with the return period evidenced by the width of the boxplots in Figure 6, the upward trend is clear for all of them, being more pronounced for the highest return period quantiles, where the increases in the precipitation quantiles reach 15% to 20%.

Again, these results align with studies from other authors (e.g., [66–68]) that predict an increase in the magnitude and frequency of extreme precipitation episodes as a consequence of climate change.

This increase in the magnitude and frequency of precipitation events is logically transferred to discharges, with these increasing significantly for all quantiles and, once again, more evidently for low-frequency quantiles. This increase in flows, however, is slightly compensated for by the decrease in the average annual precipitation and the increase in temperatures, which translate into greater evapotranspiration and lower humidity in the basin prior to storm episodes [69]. Even so, although there is a high variability between climate models, all of them predict increases in the peak discharges, which means that flood events will be more frequent and more extreme in the future.

Finally, it is worth noting the presence of the "dog-leg" effect in the flood plotting positions, as demonstrated in Figure 7 of the simulations. This distinctive phenomenon, originally described by Potter [70], is particularly evident in rivers in the Mediterranean region and can be accurately reproduced using a TCEV distribution, as proposed by Francés [71].

The escalating magnitude of extreme precipitation events underscores the imperative to urgently address and prepare for potential amplification in the scale of future river floods. As climate change continues to influence weather patterns, the heightened intensity of precipitation poses an increased risk of severe flooding. To effectively mitigate and adapt to these evolving challenges, proactive measures must be implemented. This involves not only bolstering infrastructure resilience to withstand higher water levels but also instituting comprehensive flood risk management strategies. Emphasizing the importance of early warning systems, community preparedness, and sustainable land use practices becomes paramount. Additionally, fostering international collaboration for data sharing, research, and the development of adaptive policies can play a crucial role in building a collective defense against the escalating threat of more substantial river floods. In this context, a holistic and proactive approach is essential to navigate the complex dynamics of climate-induced changes and their impact on the hydrological cycle, ensuring the safety and resilience of communities in the face of future flood events.

6. Conclusions

The increasing adoption of the SCS approach for enhancing limited hydrometeorological records relies heavily on comprehensive observational data, but often lacks temporal depth, leading to significant uncertainties in estimating flood quantiles, especially in extreme event modeling, further compounded by incorporating climate change scenarios, necessitating correction methods like the delta method or quantile mapping, yet for the accurate estimation of future flood quantiles, extending precipitation data series via a well-parameterized WG is essential. The methodology presented in Beneyto et al. [9] demonstrated that integrating additional information into the WG implementation considerably reduced the uncertainty of high-return-period flood quantile estimates when estimated by a WG. Furthermore, this was quantified under different information scenarios in Beneyto et al. [29] and in Beneyto et al. [30]. The presented methodology applied in the case study of Rambla de la Viuda draws from the premise of these studies to estimate extreme floods under climate change scenarios. In this case, the information obtained from the regionalization of the climate projections is integrated into the WG, obtaining satisfactory results.

The results obtained from the EUROCORDEX project's projections for an RCP8.5 emissions scenario in the study area analyzed show a clear increase in maximum and minimum temperatures, with more frequent and severe hot waves, which will result in increasing evapotranspiration rates. Precipitation quantiles experience similar increases to those of temperatures, although the average annual precipitation is seen to be slightly reduced. This will probably translate into a reduction in the average annual flow of rivers, combined with increasingly frequent episodes of large floods, as numerous studies already

remark. These results demonstrate the robustness of the presented methodology, being able to obtain satisfactory results at any point of the study area.

The accurate estimation of flood quantiles under climate change scenarios is of paramount importance for informed decision-making and effective water resource management. As climate patterns evolve, the frequency and intensity of extreme weather events, including floods, are anticipated to undergo significant changes. The adequate estimation of flood quantiles is crucial for assessing and mitigating the associated risks, particularly in the context of shifting precipitation patterns and altered hydrological regimes. Precise quantification enables the identification of vulnerable areas, informs the design of resilient infrastructure, and aids in the formulation of adaptive strategies. Moreover, reliable estimates are indispensable for developing robust floodplain management plans and optimizing resource allocation for flood prevention and response efforts. Inaccuracies in flood quantile estimation may lead to either underpreparedness or unnecessary investments, emphasizing the critical role of precise assessments in enhancing resilience to the challenges posed by climate change-induced variations in flood magnitudes and frequencies.

Author Contributions: Conceptualization, C.B., J.Á.A. and F.F.; data curation, C.B. and J.Á.A.; formal analysis, C.B., J.Á.A. and F.F.; investigation, C.B., J.Á.A. and F.F.; methodology, C.B., J.Á.A. and F.F.; project administration, F.F.; resources, C.B. and J.Á.A.; software, C.B. and J.Á.A.; supervision, C.B., J.Á.A. and F.F.; visualization, C.B. and J.Á.A.; writing—original draft, C.B., J.Á.A. and F.F.; writing—review and editing, C.B., J.Á.A. and F.F. All authors have read and agreed to the published version of the manuscript.

Funding: This work was supported by the Spanish Ministry of Science and Innovation through the research projects TETISCHANGE (RTI2018-093717-B-100) and TETISPREDICT (PID2022-141631OB-I00).

Data Availability Statement: The data presented in this study are available on request from the corresponding author.

Acknowledgments: The authors thank AEMET and the UC for the data provided to carry out this work (Spain02 dataset). Authors would also like to thank the Júcar River Basin Water Authority (CHJ) and its Automatic System of Hydrological Information (SAIH) for the hydrological information provided.

Conflicts of Interest: The authors declare no conflicts of interest.

References

1. Kidson, R.; Richards, K.S. Flood frequency analysis: Assumptions and alternatives. *Prog. Phys. Geogr.* **2005**, *29*, 392–410. [CrossRef]
2. Lisø, K.R.; Kvande, T.; Time, B. Climate Adaptation Framework for Moisture-resilient Buildings in Norway. *Energy Procedia* **2017**, *132*, 628–633. [CrossRef]
3. Metzger, A.; Marra, F.; Smith, J.A.; Morin, E. Flood frequency estimation and uncertainty in arid/semi-arid regions. *J. Hydrol.* **2020**, *590*, 125254. [CrossRef]
4. Soltani, A.; Hoogenboom, G. Minimum data requirements for parameter estimation of stochastic weather generators. *Clim. Res.* **2003**, *25*, 109–119. [CrossRef]
5. Merz, R.; Blöschl, G. Process controls on the statistical flood moments—A data based analysis. *Hydrol. Process.* **2009**, *23*, 675–696. [CrossRef]
6. Merz, R.; Blöschl, G. Flood frequency hydrology: 2. Combining data evidence. *Water Resour. Res.* **2008**, *44*, W08433. [CrossRef]
7. Benito, G.; Sanchez-Moya, Y.; Medialdea, A.; Barriendos, M.; Calle, M.; Rico, M.; Sopeña, A.; Machado, M.J. Extreme Floods in Small Mediterranean Catchments: Long-Term Response to Climate Variability and Change. *Water* **2020**, *12*, 1008. [CrossRef]
8. Evin, G.; Favre, A.C.; Hingray, B. Stochastic generation of multi-site daily precipitation focusing on extreme events. *Hydrol. Earth Syst. Sci.* **2018**, *22*, 655–672. [CrossRef]
9. Beneyto, C.; Aranda, J.Á.; Benito, G.; Francés, F. New approach to estimate extreme flooding using continuous synthetic simulation supported by regional precipitation and non-systematic flood data. *Water* **2020**, *12*, 3174. [CrossRef]
10. Alfieri, L.; Bisselink, B.; Dottori, F.; Naumann, G.; de Roo, A.; Salamon, P.; Wyser, K.; Feyen, L. Global projections of river flood risk in a warmer world. *Earth's Future* **2017**, *5*, 171–182. [CrossRef]
11. Paprotny, D.; Morales-Nápoles, O. Estimating extreme river discharges in Europe through a Bayesian network. *Hydrol. Earth Syst. Sci.* **2017**, *21*, 2615–2636. [CrossRef]
12. IPCC. *IPCC AR6 WGII Sixth Assessment Report*; IPCC: Geneva, Switzerland, 2022.

13. Roudier, P.; Andersson, J.C.M.; Donnelly, C.; Feyen, L.; Greuell, W.; Ludwig, F. Projections of future floods and hydrological droughts in Europe under a +2°C global warming. *Clim. Chang.* **2016**, *135*, 341–355. [CrossRef]
14. Soriano, E.; Mediero, L.; Garijo, C. Quantification of Expected Changes in Peak Flow Quantiles in Climate Change by Combining Continuous Hydrological Modelling with the Modified Curve Number Method. *Water Resour. Manag.* **2020**, *34*, 4381–4397. [CrossRef]
15. Yin, J.; Guo, S.; He, S.; Guo, J.; Hong, X.; Liu, Z. A copula-based analysis of projected climate changes to bivariate flood quantiles. *J. Hydrol.* **2018**, *566*, 23–42. [CrossRef]
16. Jain, S. Downscaling Methods in Climate Change Studies. *Nihroorkee.Gov.in* **2014**, 1–18.
17. Hay, L.E.; Wilby, R.L.; Leavesley, G.H. A comparison of delta change and downscaled GCM scenarios for three mountainous basins in the United States. *J. Am. Water Resour. Assoc.* **2000**, *36*, 387–397. [CrossRef]
18. Gleick, P.H. Methods for evaluating the regional hydrologic impacts of global climatic changes. *J. Hydrol.* **1986**, *88*, 97–116. [CrossRef]
19. Hay, L.E.; Clark, M.P. Use of statistically and dynamically downscaled atmospheric model output for hydrologic simulations in three mountainous basins in the western United States. *J. Hydrol.* **2003**, *282*, 56–75. [CrossRef]
20. Maraun, D.; Wetterhall, F.; Ireson, A.M.; Chandler, R.E.; Kendon, E.J.; Widmann, M.; Brienen, S.; Rust, H.W.; Sauter, T.; Themel, M.; et al. Precipitation downscaling under climate change: Recent developments to bridge the gap between dynamical models and the end user. *Rev. Geophys.* **2010**, *48*, RG3003. [CrossRef]
21. Pierce, D.W.; Cayan, D.R.; Maurer, E.P.; Abatzoglou, J.T.; Hegewisch, K.C. Improved bias correction techniques for hydrological simulations of climate change. *J. Hydrometeorol.* **2015**, *16*, 2421–2442. [CrossRef]
22. Mehrotra, R.; Sharma, A. A multivariate quantile-matching bias correction approach with auto- and cross-dependence across multiple time scales: Implications for downscaling. *J. Clim.* **2016**, *29*, 3519–3539. [CrossRef]
23. Themeßl, M.J.; Gobiet, A.; Heinrich, G. Empirical-statistical downscaling and error correction of regional climate models and its impact on the climate change signal. *Clim. Chang.* **2011**, *112*, 449–468. [CrossRef]
24. Maraun, D. Bias Correcting Climate Change Simulations—A Critical Review. *Curr. Clim. Chang. Rep.* **2016**, *2*, 211–220. [CrossRef]
25. Beranová, R.; Kyselý, J.; Hanel, M. Characteristics of sub-daily precipitation extremes in observed data and regional climate model simulations. *Theor. Appl. Climatol.* **2018**, *132*, 515–527. [CrossRef]
26. Faghih, M.; Brissette, F.; Sabeti, P. Impact of correcting sub-daily climate model biases for hydrological studies. *Hydrol. Earth Syst. Sci.* **2022**, *26*, 1545–1563. [CrossRef]
27. Requena, A.I.; Nguyen, T.H.; Burn, D.H.; Coulibaly, P.; Nguyen, V.T. Van A temporal downscaling approach for sub-daily gridded extreme rainfall intensity estimation under climate change. *J. Hydrol. Reg. Stud.* **2021**, *35*, 100811. [CrossRef]
28. World Meteorological Organization. *WMO Guidelines on the Calculation of Climate Normals*; WMO-No. 1203; World Meteorological Organization: Geneva, Switzerland, 2017; p. 29.
29. Beneyto, C.; Ángel, J.; Francés, F. Exploring the uncertainty of Weather Generators' extreme estimates in different practical available information scenarios. *Hydrol. Sci. J.* **2023**, *68*, 1203–1212. [CrossRef]
30. Beneyto, C.; Vignes, G.; Aranda, J.Á.; Francés, F. Sample Uncertainty Analysis of Daily Flood Quantiles Using a. *Water* **2023**, *15*, 3489. [CrossRef]
31. Camarasa, A.M.; Segura, F. Flood events in Mediterranean ephemeral streams (ramblas) in Valencia region, Spain. *CATENA* **2001**, *45*, 229–249. [CrossRef]
32. Herrera, S.; Kotlarski, S.; Soares, P.M.M.; Cardoso, R.M.; Jaczewski, A.; Gutiérrez, J.M.; Maraun, D. Uncertainty in gridded precipitation products: Influence of station density, interpolation method and grid resolution. *Int. J. Climatol.* **2019**, *39*, 3717–3729. [CrossRef]
33. Kotlarski, S.; Szabó, P.; Herrera, S.; Räty, O.; Keuler, K.; Soares, P.M.; Cardoso, R.M.; Bosshard, T.; Pagé, C.; Boberg, F.; et al. Observational uncertainty and regional climate model evaluation: A pan-European perspective. *Int. J. Climatol.* **2017**, *39*, 3730–3749. [CrossRef]
34. Meinshausen, M.; Smith, S.J.; Calvin, K.; Daniel, J.S.; Kainuma, M.L.T.; Lamarque, J.; Matsumoto, K.; Montzka, S.A.; Raper, S.C.B.; Riahi, K.; et al. The RCP greenhouse gas concentrations and their extensions from 1765 to 2300. *Clim. Chang.* **2011**, *109*, 213–241. [CrossRef]
35. Hargreaves, G.; Samani, Z. Reference Crop Evapotranspiration from Temperature. *Appl. Eng. Agric.* **1985**, *1*, 96–99. [CrossRef]
36. Gudmundsson, L.; Bremnes, J.B.; Haugen, J.E.; Engen-Skaugen, T. Technical Note: Downscaling RCM precipitation to the station scale using statistical transformations – A comparison of methods. *Hydrol. Earth Syst. Sci.* **2012**, *16*, 3383–3390. [CrossRef]
37. Haruna, A.; Blanchet, J.; Favre, A.C. Performance-based comparison of regionalization methods to improve the at-site estimates of daily precipitation. *Hydrol. Earth Syst. Sci.* **2022**, *26*, 2797–2811. [CrossRef]
38. Hosking, J.R.M.; Wallis, J.R. Some Statistics Useful in Regional Frequency Analys. *Water Resour. Res.* **1993**, *29*, 271–281. [CrossRef]
39. Hosking, J.R.M.; Wallis, J.R. *Regional Frequency Analysis: An Approach Based on L-Moments*; Cambridge University Press: New York, NY, USA, 1997; p. 238.
40. Dalrymple, T. Flood-Frequency Analyses. Manual of Hydrology Part 3. Flood-flow techniques. *Usgpo* **1960**, *1543-A*, 80.
41. Akaike, H. On Entropy Maximization Principle. In *Applications of Statistics*; Krishnaiah, P.R., Ed.; North-Holland Publishing Co.: Amsterdam, The Netherlands, 1977.

42. Papastathopoulos, I.; Tawn, J.A. Extended generalised Pareto models for tail estimation. *J. Stat. Plan. Inference* **2013**, *143*, 131–143. [CrossRef]
43. Naveau, P. Modeling jointly low, moderate, and heavy rainfall intensities without a threshold selection. *Water Resour. Res.* **2016**, *52*, 2753–2769. [CrossRef]
44. Vélez, J.J.; López Unzu, F.; Puricelli, M.; Francés, F. Parameter extrapolation to ungauged basins with a hydrological distributed model in a regional framework. *Hydrol. Earth Syst. Sci. Discuss.* **2007**, *4*, 909–956. [CrossRef]
45. Francés, F.; Vélez, J.I.; Vélez, J.J. Split-parameter structure for the automatic calibration of distributed hydrological models. *J. Hydrol.* **2007**, *332*, 226–240. [CrossRef]
46. Nash, J.E.; Sutcliffe, J. V River flow forecasting through conceptual models part I—A discussion of principles. *J. Hydrol.* **1970**, *10*, 282–290. [CrossRef]
47. Cunnane, C. Unbiased plotting positions—A review. *J. Hydrol.* **1978**, *37*, 205–222. [CrossRef]
48. Boughton, W.; Droop, O. Continuous simulation for design flood estimation—A review. *Environ. Model. Softw.* **2003**, *18*, 309–318. [CrossRef]
49. Mendoza, P.A.; McPhee, J.; Vargas, X. Uncertainty in flood forecasting: A distributed modeling approach in a sparse data catchment. *Water Resour. Res.* **2012**, *48*, W09532. [CrossRef]
50. Sankarasubramanian, A.; Lall, U. Flood quantiles in a changing climate: Seasonal forecasts and causal relations. *Water Resour. Res.* **2003**, *39*, 1134. [CrossRef]
51. Gu, L.; Yin, J.; Zhang, H.; Wang, H.M.; Yang, G.; Wu, X. On future flood magnitudes and estimation uncertainty across 151 catchments in mainland China. *Int. J. Climatol.* **2021**, *41*, E779–E800. [CrossRef]
52. Moradkhani, H. Hydrologic remote sensing and land surface data assimilation. *Sensors* **2008**, *8*, 2986–3004. [CrossRef] [PubMed]
53. Pumo, D.; Francipane, A.; Cannarozzo, M.; Antinoro, C.; Noto, L.V. Monthly Hydrological Indicators to Assess Possible Alterations on Rivers' Flow Regime. *Water Resour. Manag.* **2018**, *32*, 3687–3706. [CrossRef]
54. Gibson, C.A.; Meyer, J.L.; Poff, N.L.; Hay, L.E.; Georgakakos, A. Flow regime alterations under changing climate in two river basins: Implications for freshwater ecosystems. *River Res. Appl.* **2005**, *21*, 849–864. [CrossRef]
55. Schneider, C.; Laizé, C.L.R.; Acreman, M.C.; Flörke, M. How will climate change modify river flow regimes in Europe? *Hydrol. Earth Syst. Sci.* **2013**, *17*, 325–339. [CrossRef]
56. Devkota, L.P.; Gyawali, D.R. Impacts of climate change on hydrological regime and water resources management of the Koshi River Basin, Nepal. *J. Hydrol. Reg. Stud.* **2015**, *4*, 502–515. [CrossRef]
57. Mengistu, D.; Bewket, W.; Dosio, A.; Panitz, H.J. Climate change impacts on water resources in the Upper Blue Nile (Abay) River Basin, Ethiopia. *J. Hydrol.* **2021**, *592*, 125614. [CrossRef]
58. Gosling, S.N.; Arnell, N.W. A global assessment of the impact of climate change on water scarcity. *Clim. Chang.* **2016**, *134*, 371–385. [CrossRef]
59. Hartmann, D.L. Global Climate Models. In *Global Physical Climatology*; Elsevier: Amsterdam, The Netherlands, 2016; pp. 325–360.
60. Randall, D.A.; Wood, R.A.; Bony, S.; Colman, R.; Fichefet, T.; Fyfe, J.; Kattsov, V.; Pitman, A.; Shukla, J.; Srinivasan, J.; et al. Chapter 8: Climate Models and Their Evaluation. In *Climate Change 2007: The Physical Science Basis. Contribution of Working Group I to the Fourth Assessment Report of the Intergovernmental Panel on Climate Change*; Cambridge University Press: Cambridge, UK, 2007; Available online: https://www.researchgate.net/publication/233421523_Climate_Models_and_Their_Evaluation (accessed on 2 December 2023).
61. Flato, G.; Marotzke, J.; Abiodun, B.; Braconnot, P.; Chou, S.C.; Collins, W.; Cox, P.; Driouech, F.; Emori, S.; Eyring, V.; et al. *Evaluation of climate models. Climate Change 2013 the Physical Science Basis: Working Group I Contribution to the Fifth Assessment Report of the Intergovernmental Panel on Climate Change*; Cambridge University Press: Cambridge, UK, 2013; pp. 741–866.
62. Wuebbles, D.J.; Fahey, D.W.; Hibbard, K.A.; De Angelo, B.; Doherty, S.; Hayhoe, K.; Horton, R.; Kossin, J.P.; Taylor, P.C.; Waple, A.M.; et al. Executive summary. In *Climate Science Special Report: Fourth National Climate Assessment*; U.S. Global Change Research Program: Washington, DC, USA, 2017; Volume 16, pp. 193–205.
63. Zubaidi, S.L.; Kot, P.; Hashim, K.; Alkhaddar, R.; Abdellatif, M.; Muhsin, Y.R. Using LARS-WG model for prediction of temperature in Columbia City, USA. *IOP Conf. Ser. Mater. Sci. Eng.* **2019**, *584*, 012026. [CrossRef]
64. Guerreiro, S.B.; Dawson, R.J.; Kilsby, C.; Lewis, E.; Ford, A. Future heat-waves, droughts and floods in 571 European cities. *Environ. Res. Lett.* **2018**, *13*, 034009. [CrossRef]
65. Lhotka, O.; Kyselý, J.; Farda, A. Climate change scenarios of heat waves in Central Europe and their uncertainties. *Theor. Appl. Climatol.* **2018**, *131*, 1043–1054. [CrossRef]
66. Prein, A.F.; Rasmussen, R.M.; Ikeda, K.; Liu, C.; Clark, M.P.; Holland, G.J. The future intensification of hourly precipitation extremes. *Nat. Clim. Chang.* **2017**, *7*, 48–52. [CrossRef]
67. Wasko, C.; Nathan, R.; Stein, L.; O'Shea, D. Evidence of shorter more extreme rainfalls and increased flood variability under climate change. *J. Hydrol.* **2021**, *603*, 126994. [CrossRef]
68. Willems, P.; Vrac, M. Statistical precipitation downscaling for small-scale hydrological impact investigations of climate change. *J. Hydrol.* **2011**, *402*, 193–205. [CrossRef]
69. Teuling, A.J.; De Badts, E.A.G.; Jansen, F.A.; Fuchs, R.; Buitink, J.; Van Dijke, A.J.H.; Sterling, S.M. Climate change, reforestation/afforestation, and urbanization impacts on evapotranspiration and streamflow in Europe. *Hydrol. Earth Syst. Sci.* **2019**, *23*, 3631–3652. [CrossRef]

70. Potter, W.D. Upper and lower frequency curves for peak rates of runoff. *Eos Trans. Am. Geophys. Union* **1958**, *39*, 100–105. [CrossRef]
71. Francés, F. Using the TCEV distribution function with systematic and non-systematic data in a regional flood frequency analysis. *Stoch. Hydrol. Hydraul.* **1998**, *12*, 267–283. [CrossRef]